






Original Article

Effect of stress paths on failure mechanism and progressive damage of hard-brittle rock

CHEN Zi-quan^{1,2,3}  <https://orcid.org/0000-0002-8652-7561>; e-mail: chenziqun@swjtu.edu.cn

HE Chuan¹  <https://orcid.org/0000-0003-3551-5314>; e-mail: chuanhe12@163.com

HU Xiong-yu^{1*}  <https://orcid.org/0000-0001-6536-9229>;  e-mail: srock89@163.com

MA Chun-chi^{1,3}  <https://orcid.org/0000-0002-5852-8022>; e-mail: machunchi17@cdut.edu.cn

*Corresponding author

¹ Key Laboratory of Transportation Tunnel Engineering, Ministry of Education, Southwest Jiaotong University, Chengdu 610031, China

² Key Laboratory of Engineering Structures of Heavy Haul Railway, Ministry of Education, Central South University, Changsha 410075, China

³ State Key Laboratory of Geohazard Prevention and Geoenvironment Protection, Chengdu University of Technology, Chengdu 610059, China

Citation: Chen ZQ, He C, Hu XY, Ma CC (2021) Effect of stress paths on failure mechanism and progressive damage of hard-brittle rock. Journal of Mountain Science 18(9). <https://doi.org/10.1007/s11629-020-6554-9>

© Science Press, Institute of Mountain Hazards and Environment, CAS and Springer-Verlag GmbH Germany, part of Springer Nature 2021

Abstract: During deep buried hard-brittle rock tunnel excavation, the surrounding rock experiences a complicated stress path and stress adjustment process. Once the adjusted stress exceeds the ultimate bearing capacity of rockmass, a rock failure mode defined as stress-cracking type will occur. In order to investigate the effect of stress paths on failure mechanism and progressive damage of deep-buried rockmass, the cyclic loading-unloading, loading-unloading, uniaxial, conventional and unloading triaxial compression tests on samples of hard-brittle sandstone were conducted. According to the experimental results, increase in the confining pressure was beneficial to improve the mechanical parameters of rock, but it will reduce the brittle failure features. Compared with conventional triaxial compression, the sandstone under unloading state had more remarkable stress drop and unstable failure characteristics. Meanwhile, it was found that the energy dissipation and energy release in the whole process of rock deformation were the internal power of driven rock progressive damage. With the increase

of confining pressure, the energy hardening and energy accumulation features of rock were weakened, while the progressive damage evolution characteristics could be enhanced. In unloading state, more energy could be converted into elastic energy in the energy softening phase ($\sigma_{eb}-\sigma_P$), so that the pre-peak damage rate of rock was lower than that of conventional triaxial compression state. Thus, the energy dissipation rate of rock after peak strength decreased linearly with the increase of confining pressure under conventional triaxial compression state, while in unloading state it showed the opposite law.

Keywords: Hard-brittle rock; Stress path; Confining pressure; Failure mechanism; Progressive damage

1 Introduction

With the continuous development of China's transportation and hydropower projects to the western mountainous areas, more and more

Received: 27-Oct-2020
Revised: 31-Jan-2021
Accepted: 12-May-2021

underground engineering have been or will be built in the deep buried hard-brittle rockmass, and the largest buried depth can even reach 2500 m. Together with the strong tectonic stress formed by the compression of Qinghai-Tibet plateau in this region, once the rockmass is excavated into the deep stratum, complicated high geo-stress environment become the common feature of the deep underground engineering. Meanwhile, the hard-brittle rockmass has good energy storage capacity under the deep-buried stratum, and high releasable elastic strain energy could be stored before tunnel construction (Chen et al. 2017; Huang and Li 2014; Li et al. 2017; Ma et al. 2016). Large-scale excavation of high energy-storing rockmass will result in strong initial geo-stress disturbance, which could induce continuous squeezing large deformation or sudden brittle failure of surrounding rock (Barla et al. 2011; Dwivedi et al. 2013; Feng et al. 2016). For this reason, the failure mechanism and progressive damage of hard-brittle rock under high geo-stress and their influence on tunnel excavation have become a hot and difficult problem in the field of engineering geology and rock mechanics (Liu et al. 2016; Ma et al. 2020; Xiao et al. 2016).

During the excavation of the deep-buried hard rock tunnel, the stress unloading effect will break the original balance of its three-dimensional stress state, resulting in the redistribution of the internal stress field. In this process, the surrounding rock of the tunnel has to undergo a series of complex stress paths, especially the rockmass near the excavation face (Cantièni and Anagnostou 2009; Diederichs et al. 2004; Lim and Ou 2017; Li et al. 2014). The mechanical behavior of the rockmass depends on the change of stress state. Under different stress paths, both the mechanical parameters of rock and its failure mechanism will change significantly (Chen et al. 2019; Hua and You 2001; Khazaei et al. 2015; Munoz et al. 2016). Commonly, the damage mechanism of unloading and loading caused by excavation of rockmass is totally different from that in continuous loading state. At the same time, the increase of buried depth and initial geo-stress could also change the failure mode and progressive damage mechanism of rockmass (Cui et al. 2019; Li et al. 2017; Yan et al. 2015). By laboratory test, it has been founded that the failure mode and fracture mechanism of rock will be affected by the confining pressure level and unloading rate. With the increase of unloading rate, the failure of

rock will gradually transition from shear failure to tension failure. The larger the initial confining pressure and the unloading rate is, the more serious the phenomenon of rock debris splashing will be (Xu et al. 2019; Yang 2016). However, the failure mechanism and progressive damage of rock under different stress paths need to be further investigated from more analytical perspectives (e.g. acoustic emission, energy damage evolution theory, CT scanning, etc.), especially for hard-brittle rock, which is of great significance to study the rockburst disaster mechanism in deep-buried tunnel under high geo-stress.

In this paper, an MTS815 rock mechanics test system and a PCI-II acoustic emission device were used to conduct cyclic loading-unloading, loading-unloading, uniaxial, conventional and unloading triaxial compression tests on samples of sandstone. The hard-brittle rock was retrieved at a buried depth of 720 m from the Bamiao tunnel in Sichuan province, China, where the measured maximum in-situ stress was up to 25.3 MPa and strong rockburst disaster frequently occurred in the process of tunnel construction. According to the experimental results, the effect of stress path and confining pressure on mechanical properties and failure mechanism of deep-buried rock were systematically discussed. Meanwhile, using energy damage theory and acoustic emission, the progressive damage evolution characteristics and evolution rate of hard-brittle sandstone under different stress paths were investigated.

2 Engineering Background And Experimental Method

2.1 Engineering background

According to the altitude distribution, the Chinese mainland can be generally divided into three levels, namely, the first ladder (average altitude 4500 m), the second ladder (average altitude 1000~2000 m) and the third ladder (average altitude 500 m). As shown in Fig. 1, the Bamiao tunnel is located in the transition zone between the first ladder and the second ladder of China. Suffered by the tectonic compression from the Qinghai-Tibet plateau to the eastern Yangtze platform in Sichuan Province, the results of geo-stress back analysis revealed that the

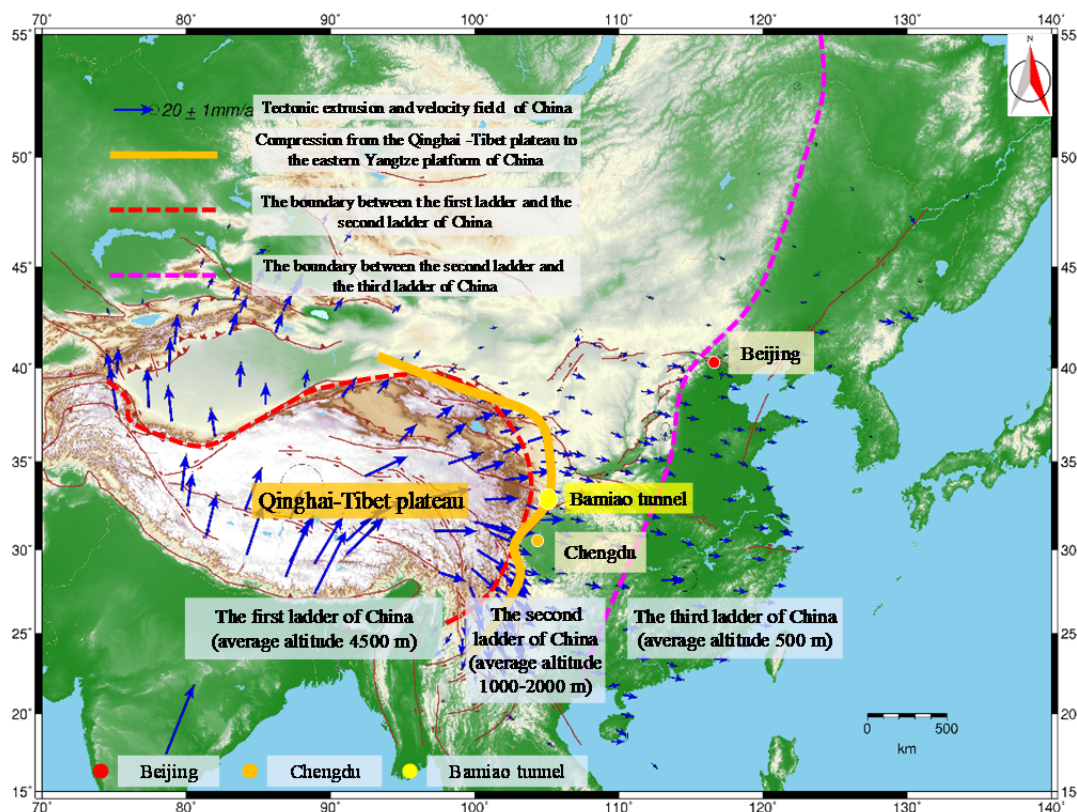


Fig. 1 Regional geological background of Bamiao tunnel, in Sichuan province, China.

maximum geo-stress of the Bamiao tunnel was up to 25~35 MPa at a buried depth of 850 m. Meanwhile, the lithology of the Bamiao tunnel was mainly composed of hard sandstone and diorite ($\sigma_c > 120$ MPa). These hard-brittle rocks could store a lot of releasable elastic strain energy under high geo-stress environment. Before tunnel excavation, the deep-buried rockmass was in a very complicated three-dimensional stress state. With the excavation of the tunnel, the surrounding rock on both sides could be turned into a two-dimensional compression stress state (Fig. 2).

Under high in-situ stress environment, the rapid adjustment of the stress paths was the key factor affecting the stability of surrounding rock. This process was accompanied by the gradual evolution of rock internal fracture and the rapid release of elastic strain energy. The failure mechanism of rock is determined by the change path of rock stress state and its mechanical properties. Commonly, for the soft-rock tunnel, the surrounding rock excavation under high geo-stress was easy to induce the squeezing large deformation. As for hard-brittle rock tunnel, it was more likely to encounter dynamic failure disaster represented by rockburst. Hence,

under the combined action of high geo-stress environment and complex stress paths, plus the hard-brittle sandstone possesses good energy storage capacity, the Bamiao tunnel frequently encountered rockburst disaster during its construction period (Fig. 3).

2.2 Experimental method

During the excavation of the deep-buried

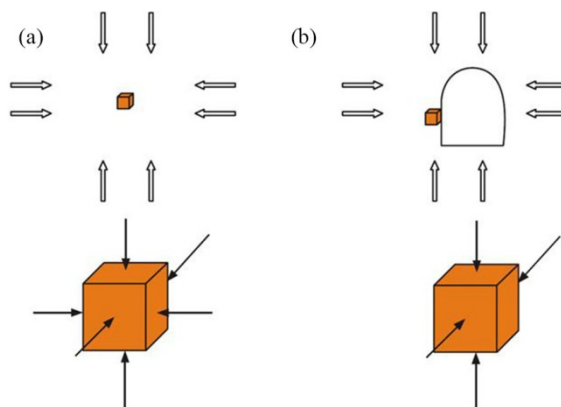


Fig. 2 The stress state of rockmass before (a) and after (b) tunnel excavation.

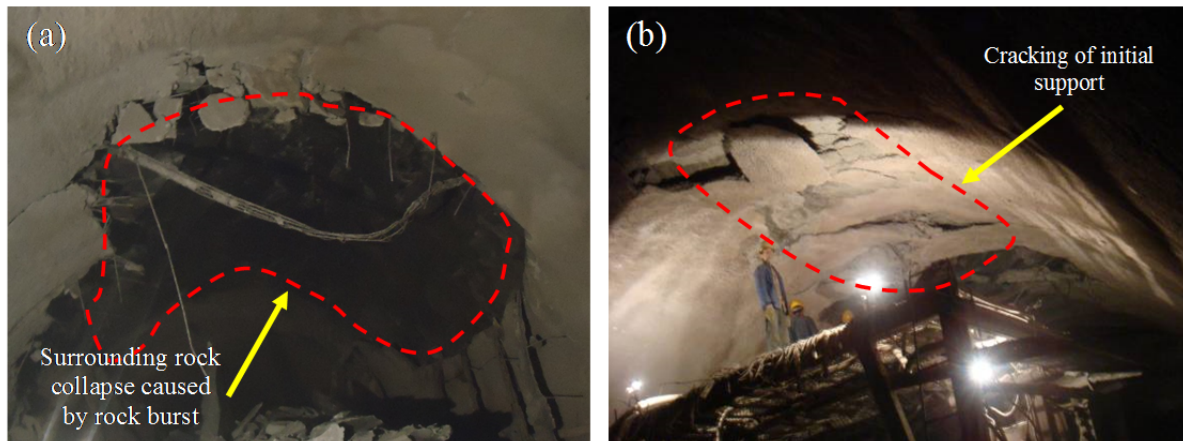


Fig. 3 Rockburst disasters happened in Bamiao tunnel.

Table 1 Mechanical parameters of sandstone under different stress paths

Samples number	Test type	Confining pressure (MPa)	Peak strength (MPa)	Peak strain (%)	σ_{cd}/σ_P	E (GPa)	μ
B-0	loading-unloading	0	-	-	-	31.96	0.077
D-0	uniaxial	0	171.9	0.49	76.1%	32.38	0.076
S-20	conventional triaxial	20	270.4	0.72	78.4%	47.94	0.127
S-30	conventional triaxial	30	317.7	0.84	79.5%	52.32	0.135
S-40	conventional triaxial	40	359.9	1.02	83.0%	56.59	0.139
X-20	unloading triaxial	20	255.9	0.98	87.5%	29.61	0.105
X-30	unloading triaxial	30	307.6	1.16	86.4%	32.26	0.122
X-40	unloading triaxial	40	338.1	1.26	84.7%	34.95	0.136
C-40	cyclic loading-unloading	40	321.5	1.46	-	-	-

Note: σ_{cd} , the crack damage stress threshold; σ_P , peak strength; E , elastic modulus; μ , Poisson's ratio.

rockmass under high geo-stress environment, the surrounding rock near the tunnel face undergoes a complex stress path in the processes of stress field redistribution. Under the unloading stress path, the rockmass with high in-situ stress shows different mechanical behavior from that under loading stress path, which often leads to large deformation, rockburst and other engineering disasters. Thus, in order to investigate the effect of stress paths on failure mechanism and progressive damage of hard-brittle rock under different confine pressures, we conducted cyclic loading-unloading, loading-unloading, uniaxial, conventional and unloading triaxial compression tests on sandstone from the Bamiao tunnel. All samples were retrieved at a buried depth of 720 m, where the measured maximum in-situ stress was up to 25.3 MPa. And they were prepared according to the methodology suggested by the International Society of Rock Mechanics and Rock Engineering (ISRM) with diameters of 50 mm and heights of 100 mm ($\varphi 50$ mm \times 100 mm). Considering the layered sedimentary structure of sandstone, all samples with a uniform bedding angle of $\beta=0^\circ$ were cored by drilling bit

perpendicular to the sedimentary surface. From the x-ray diffraction and polarized scanning tests, it was found that the minerals of sandstone were mainly quartz, plagioclase, chlorite, calcite and illite, and their proportions were 52%, 13%, 12%, 14% and 9%, respectively. Among them, brittle mineral particles represented by quartz and plagioclase accounted for a large proportion.

All rock compression tests were carried out by the MTS815 rock mechanics test system and PCI- II acoustic emission device. Table 1 shows the experimental conditions, cyclic loading-unloading, loading-unloading, uniaxial, conventional triaxial and unloading triaxial compression tests on hard-brittle sandstone were conducted. Among them, the cyclic loading-unloading test was used to verify the energy driven progressive damage mechanism of rock. In order to analyze the damage evolution mechanism of deep buried rockmass, the confining pressure in triaxial compression tests was set at 20, 30 and 40 MPa. Meanwhile, the stress unloading point of B-0, X-20, X-30 and X-40 were 70% of the peak strength of D-0, S-20, S-30 and S-40 accordingly. In order to

more accurately capture the acoustic emission signal in the process of rock damage evolution, a total of 8 AE sensors were arranged. In uniaxial compression test, the sensors were attached to the rock, while in triaxial test, the sensors were attached to the triaxial chamber. The sampling frequency of the AE system was set to 5 MHz, and the threshold of recording was 40 dB.

3 Effect of Stress Paths on Failure Mechanism

3.1 Uniaxial compression tests

The whole process of uniaxial compression test was to apply axial load on the hard-brittle sandstone specimen under unconfined condition, from the initiation, propagation, extension, coalescence of micro cracks to the post-peak failure stage. Stress and strain data were acquired throughout the testing processes, a lateral deformation rate control mode of 0.03 mm/min was adopted. The stress-strain curves and failure characteristics in uniaxial compression tests were shown in Fig. 4. Both of the B-0 and D-0 exhibited significant mechanical behavior of hard-brittle rock, the shape of stress-strain curves belonged to unstable failed type. Through the loading-unloading compression curve of B-0, the rockburst proneness *Wet* (i.e. the ratio of dissipated strain energy to elastic strain energy) could be obtained. Based on the calculation results, the *Wet* of sandstone from Bamiao tunnel was up to 2.6, which belong to medium rockburst intensity. And the peak strength of sandstone reached 171.9 MPa, whereas the strain corresponding to peak strength was only 0.49%.

From the evolution law of stress and strain, the sandstone had slight initial crack compaction deformation characteristics. However, with the increase of stress, it soon entered into the stage of elastic deformation. When the axial stress exceeded the crack damage stress threshold σ_{cd} of 130.7 MPa, the rock changed from volume compression to volume expansion as the circumferential strain began to show nonlinear characteristics (Martin and Chandler 1994). After the stress reached 158.3 MPa, the sandstone gradually entered the elastic-plastic deformation stage. Then macro fracture occurred quickly, and the stress dropped rapidly as the typical hard-brittle rock. It can be seen from the failure characteristics that the failure mechanism of sandstone was mainly vertical tension fracture, and brittle crack sounds were accompanied when it was destroyed.

3.2 Conventional triaxial compression tests

In the conventional triaxial compression tests, the confining pressure was increased to a predetermined value at first (20, 30 and 40 MPa), then kept constant and increased the axial load continuously until the rock entered the residual deformation stage. The control mode still adopted the lateral deformation rate control mode of 0.03 mm/min. Fig. 5 shows the stress-strain curves and failure characteristics. Due to the compaction effect of confining pressure, the initial crack deformation characteristics were basically disappeared. With the continuous increases of stress, sandstone gradually entered the elastic-plastic deformation stage. When the stress reached its peak strength, it showed significant stress drop characteristics under different

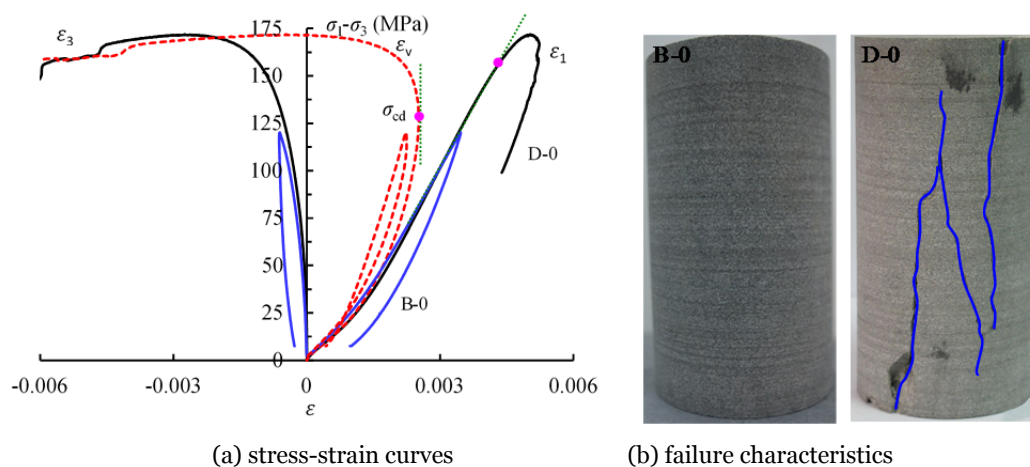


Fig. 4 Stress-strain curves and failure characteristics in uniaxial compression tests.

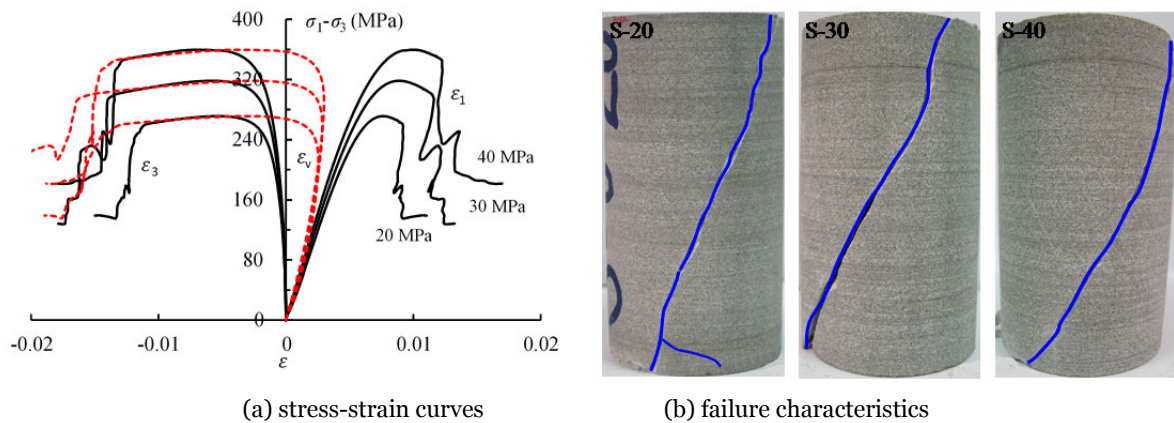


Fig. 5 Stress-strain curves and failure characteristics in conventional triaxial compression tests

confining pressures. Compared with uniaxial condition, the sandstone under different confining pressures had more remarkable pre-peak plastic deformation and shear failure feature. With the increase of confining pressure, the peak strength and peak strain of rock increased gradually. Under confining pressure of 20, 30 and 40 MPa, the elastic modulus of sandstone were 47.94, 52.32 and 56.59 GPa, which were 48.1%, 61.6% and 74.7% higher than that of uniaxial compression test. However, as the rock was under triaxial compression state, the stress drop and unstable failure characteristics in the post-peak stage decreased, and it was more significant with the increase of confining pressure.

At the same time, with the increase of confining pressure, the crack damage stress and its ratio to peak strength (σ_{cd}/σ_p) increased gradually. Which means that the fracture damage evolution of rock would go through a longer process. Hence, it could be seen from the failure characteristics, the tensile failure features of sandstone basically disappeared, showing a single shear macro fracture. Under confining pressure of 20, 30 and 40 MPa, the failure angles of sandstone were about 69°, 64° and 58°, respectively. Under high confining pressure state, the mechanical parameters and failure angle of rock increased gradually, but the brittle failure characteristics of rock weakened gradually.

3.3 Unloading triaxial compression tests

During rockmass excavation process, the surrounding rock pressure around the tunnel could be redistributed and readjusted. On the one hand, the radial stress gradually decreases with the approach to the free surface, and drops to zero at the tunnel wall.

On the other hand, the tangential stress increases with the approach to the free surface, reach its maximum value at the tunnel wall (Fig. 2). In general, this process of complex stress state change caused by excavation and unloading of tunnel can be simulated by means of laboratory test of reducing confining pressure and increasing axial pressure. Thus, in order to analyze the influence of unloading stress path on rock failure mechanism, unloading triaxial compression tests under different initial confining pressures were carried out. The unloading point of sandstone was set as 70% of the peak strength of conventional triaxial compression test under the same confining pressure. Experimental control method before unloading point was consistent with the conventional test. When the stress value reached the unloading point, it began to release the confining pressure at a rate of 0.5 MPa/min. At the same time, the axial pressure was also controlled by the lateral deformation rate control mode of 0.03 mm/min.

The stress-strain curves and failure characteristics in unloading triaxial compression tests were presented in Fig. 6. The mechanical behavior of rock before unloading point was consistent with that of conventional triaxial compression test. Once the hard-brittle sandstone entered the unloading deformation stage, its plastic deformation features began to strengthen. From the shape of the stress-strain curves, compared with the conventional triaxial compression tests, the elastic-plastic deformation characteristics during pre-peak stage were reduced, and the stress drop features at the post-peak stage were enhanced. Under confining pressure of 20, 30 and 40 MPa, the peak strength of sandstone was 255.9, 307.6 and 338.1 MPa, respectively. Reduced by 5.3%, 3.2% and 6.1% when compared with the

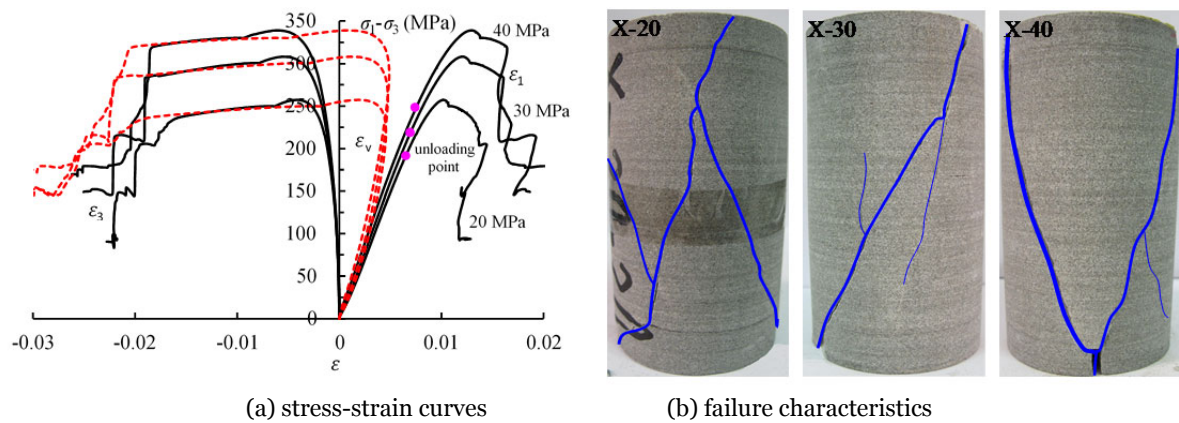


Fig. 6 Stress-strain curves and failure characteristics in unloading triaxial compression tests

conventional triaxial compression tests under the same confining pressure, whereas the peak strain increased by 36.1%, 38.1%, 23.5%. Resulting in the elastic modulus of sandstone under unloading state was reduced. Nevertheless, the σ_{cd}/σ_P of X-20, X-30 and X-40 were 87.5%, 86.4% and 84.7%, higher than that under conventional triaxial compression condition. In addition, the smaller the confining pressure was, the later the rock entered the crack damage evolution stage, which made the rock failure more sudden. Moreover, according to the failure characteristics of sandstone, the brittle failure characteristics under unloading stress path were enhanced. Compared with the conventional triaxial test, its shear feature was weakened, but its tensile failure mechanism was enhanced. The angle of main macro-fracture was lower than that of conventional triaxial state. Besides, several secondary cracks were formed during the unloading process.

4 Effect of Stress Paths on Progressive Damage

4.1 Energy theory of rock

It has been accepted extensively that the damage evolution and final unstable failure of rock are driven by energy (Chen et al. 2019; Huang and Li 2014). The energy mechanism of rock composed of energy hardening effect and energy softening effect, which the first one increases the mechanical properties of rock and embodied as energy accumulation, whereas the second one decreases the mechanical properties and presented as energy dissipation. To investigate the progressive damage evolution characteristics of

rock under different stress paths, rock energy theory and acoustic emission technique were adopted in this paper. As shown in Fig. 7, based on the energy mechanism, the deformation and failure of the rock are accompanied by energy inputting, energy accumulation, energy dissipation and energy release. The strain energy of the rock can be divided into three kinds, i.e., U , which denotes the total energy absorbed by the rock; U_e , which represents the elastic strain energy stored in the rock; and U_d , which represents the dissipated energy that is responsible for plastic deformation and crack propagation. The computational expression for the U and U_e are as follows (Xie et al. 2005):

$$U = U_e + U_d \tag{1}$$

$$U = \int \sigma_1 d\epsilon_1 + 2 \int \sigma_3 d\epsilon_3 + \frac{3(1-2\nu_0)}{2E_0} (\sigma_3^0)^2 \tag{2}$$

$$U_e = \frac{1}{2E_u} [\sigma_1^2 + 2\sigma_3^2 - 2\nu_u (\sigma_3^2 + 2\sigma_1\sigma_3)] \tag{3}$$

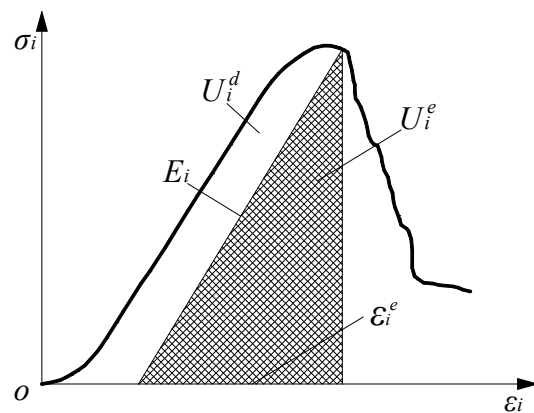


Fig. 7 Relationship between elastic strain energy and dissipated energy in rock.

where E_0 , E_u , ν_0 , and ν_u are the initial elasticity modulus, unloading elastic modulus, initial Poisson's ratio, and the unloading Poisson's ratio, σ_3^0 of the initial confining pressure.

In order to study the progressive damage evolution mechanism of rock, a cyclic loading and unloading test of C-40 on the sandstone was conducted. The confining pressure was first increased to 40MPa, and the increment of each cycle was 20MPa. In the elastic stage, the axial loading rate was 1.0 MPa/s, as the rock entered the elastic-plastic deformation stage, the control mode gradually changed to the circumferential strain of 0.02 mm/min. Suffered by the progressive damage and deterioration caused by cyclic loading and unloading, the peak strength of C-40 decreased to 321.5 MPa, which was 89.3% of S-40 and 95.1% of X-40. Fig. 8 shows the evolution curves of dissipated energy, in each loading process, the dissipated energy of rock increased gradually. While in each unloading process, the dissipated energy of rock reduced. The higher the load level, the more strain energy of the rock dissipated. When the rock entered the failure stage, the dissipated energy could suddenly increase sharply. Therefore, the evolution law of dissipated energy could verify that the damage of rock was driven by energy, and it could reflect the progressive damage evolution process of rock. The mechanism of fracture evolution and energy dissipation of rock specimen was the same as that of stress wave released by surrounding rock damage

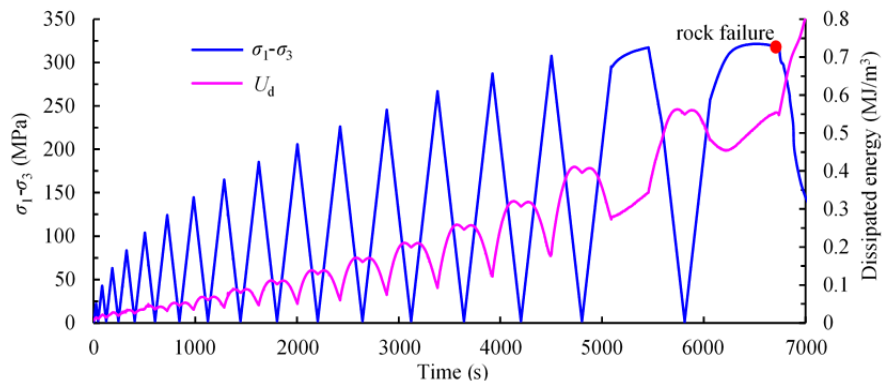


Fig. 8 Evolution curves of dissipated energy in the cyclic loading and unloading test.

during tunnel excavation. As presented in Fig. 9, acoustic emission event (i.e. the strain energy dissipated in the process of rock fracture) was the elastic wave release phenomenon of initiation, propagation, extension, coalescence of micro cracks and the internal damages of rock under the action of external pressure. For tunnels, the deep buried rockmass with good energy storage capacity could accumulate a lot of elastic strain energy before excavation. During the tunnel excavation and surrounding rock deformation processes, the strain energy would gradually dissipate and lead to rock damage. This is the energy mechanism of rockburst disaster easily induced during the excavation of deep buried hard-brittle rockmass.

4.2 Progressive damage characteristics

Energy dissipation and release in the process of rock deformation were the internal power of driven rock progressive damage. Fig. 10 shows the damage evolution characteristics of sandstone under loading-unloading condition, which include the strain energy, strain energy ratio (i.e. $P_e=U_e/U$ and $P_d=U_d/U$) and

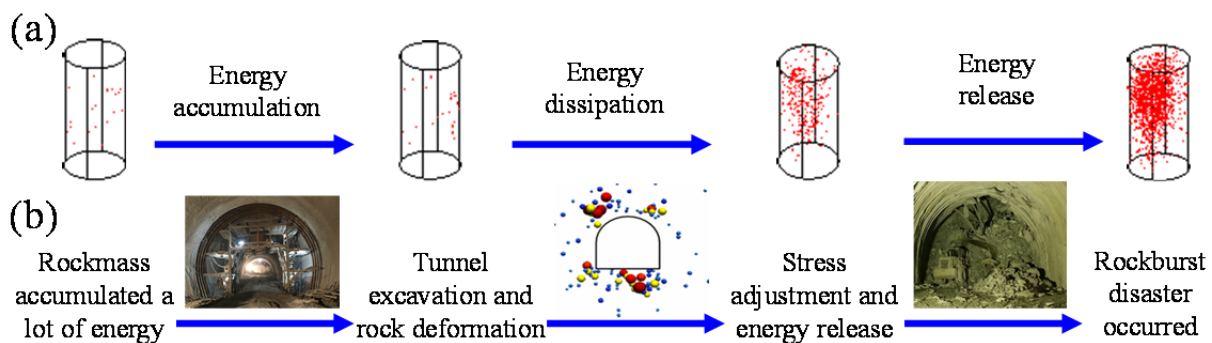


Fig. 9 Energy evolution mechanism of rockmass during tunnel excavation: (a) AE evolution of rock; (b) microseismic signal and surrounding rock failure.

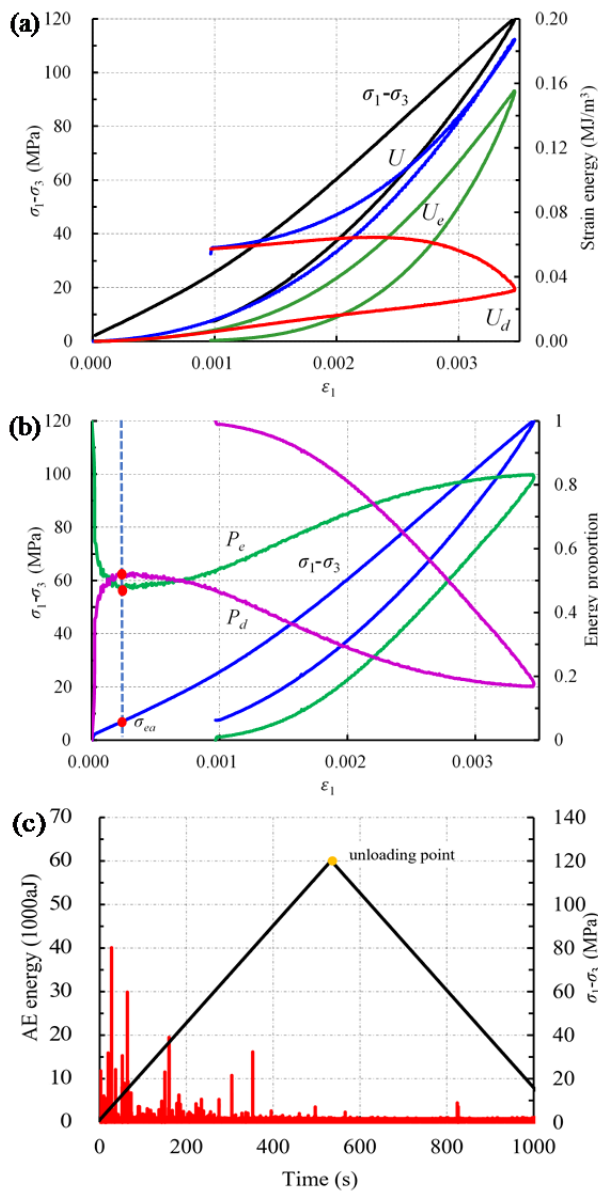


Fig. 10 Progressive damage evolution characteristics of B-o: (a) strain energy; (b) strain energy ratio; (c) acoustic emission.

acoustic emission evolution curves. At the initial loading stage, the proportion of dissipated energy to total energy increased rapidly, while the elastic energy ratio decreased quickly. This stage was mainly the original micro-cracks compression and mutual occlusion of mineral particles in rock. As the rock entered the linear elastic deformation stage, the dissipation energy and elastic energy kept stable growth. It was the main energy storage stage, most of the energy absorbed by rock was converted into releasable elastic energy and stored inside. Hence, once the pressure on the rock is unloading gradually,

the U_e and P_e will decrease with the stress. But the dissipated energy was irreversible, which lead to the accumulation of damage in rock. Consistent with the strain energy evolution law, acoustic emission can also reflect the gradual damage process of rock. The internal fracture mechanism presented the foreshock-slight shock type under the stress path of loading-unloading. Main AE events were concentrated in the initial crack compression stage, and there were almost no AE events in the subsequent linear elastic stage and unloading stage.

Through the above analysis, it can be seen that the strain energy, strain energy ratio and acoustic emission evolution curves could combined express the energy transfer mechanism and the progressive damage evolution law of rock in the process of loading and unloading. Thus, failure tests under different stress paths were carried out and Fig. 11 shows the progressive damage evolution characteristics of D-o. According to the S-shaped evolution law of strain energy ratio (P_e and P_d), two stress thresholds, σ_{ea} and σ_{eb} , can be obtained. Which could be considered as the threshold points for rock entering the energy hardening stage and energy softening stage (Chen et al. 2019). Thus, the progressive damage evolution process of deep-buried sandstone can be divided into the following four phases:

(1) The initial compression phase ($0 - \sigma_{ea}$): from 0 to 11.1 MPa, the rock did not absorb much energy, 54.9% of which was dissipated in the process of compaction and closure of primary cracks, and the remaining 45.1% was stored in the form of elastic strain energy. Similar to the loading phase of B-o, many low-level AE events were generated at this stage, the maximum AE energy value were 78.3×10^3 aJ.

(2) The energy hardening phase ($\sigma_{ea} - \sigma_{eb}$): from 11.1 to 140.4 MPa, the energy proportion exhibit an energy-hardening phenomenon in which P_e gradually increased and P_d gradually decreased. This is the main energy storage stage of the rock, the elastic energy kept growing in line with the total energy, and hardly any AE events in this phase. At the stress threshold of σ_{eb} , the elastic strain energy accounted for 94.8% of the total energy, while the dissipated energy only accounted for 5.2% under uniaxial compression.

(3) The energy softening phase ($\sigma_{eb} - \sigma_f$): from 140.4 to 171.9 MPa, as the stress exceeded the σ_{eb} , the elastic energy curve started to deviate from the total energy curve. Internal fracture and damage of rock began to accelerate. With the increases of stress, the

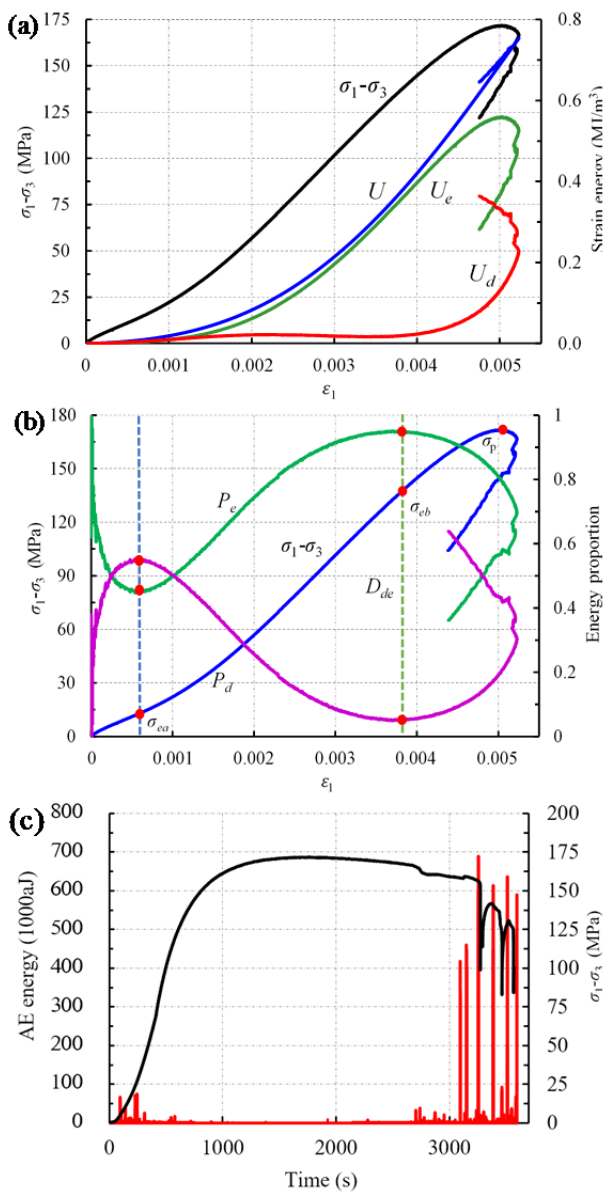


Fig. 11 Progressive damage evolution characteristics of D-o: (a) strain energy; (b) strain energy ratio; (c) acoustic emission.

dissipated energy increased nonlinearly. Thus, the elastic energy proportion decreased gradually, while the dissipated energy proportion increased steadily. As the energy mechanism of hard-brittle rock was still dominated by energy accumulation ($P_e > 0.8$), only few acoustic emission events occurred at this stage. However, in the later stage of elastic-plastic deformation, AE events began to increase with the increased of internal fracture in sandstone.

(4) The post-peak phase (σ_p): from 171.9 MPa to residual strength, once the hard-brittle rock entered this failure stage, the elastic strain energy could be

released suddenly, and the acoustic emission events increased abruptly. Thus, the dissipated energy proportion increased gradually and exceeded that of elastic energy. The maximum AE energy value of sandstone up to remarkable 689.2×10^3 aJ under the stress path of uniaxial compression.

In general, the energy damage evolution mechanism of hard brittle sandstone in the pre-peak stage was mainly energy accumulation, and it changed into energy release in the post-peak stage and had a strong brittle failure characteristic. Thus, the AE events in the whole process of deformation under uniaxial compression stress path was shown as the slight shock-no shock-main shock type.

Under triaxial compression stress state, rocks have higher strength and can gather more energy, but the confining pressure effect will change its damage evolution characteristics. The plastic failure characteristics of rock will gradually increase with the increase of confining pressure. Especially under the extremely high confining pressure state, the post-peak deformation of rock may present as ideal plasticity. Even though, the rockburst disaster in hard-brittle rockmass was mostly concentrated in deep buried condition. Hence, in order to study the effect of high confining pressure on the damage mechanism of hard-brittle rock, taking S-40 as an example, Fig. 12 shows its progressive damage evolution characteristics.

Benefit from the compaction effect of high confining pressure loading, the initial compression phase ($0-\sigma_{ea}$) was basically disappeared, and the rock entered the linear elastic deformation stage earlier. The σ_{ea}/σ_c and P_e at stress σ_{ea} of S-40 was 7.2% and 54.5%, respectively. After entering the energy hardening phase ($\sigma_{ea}-\sigma_{eb}$), the elastic energy began to increase, and the total energy done by the external force in this stage was almost stored in the form of elastic energy. The cracks in the rock had not yet started to sprout, showing the characteristics of strain hardening and energy accumulation. When the stress exceeded the σ_{eb} , the bifurcation of the elastic energy and the total energy curves indicated that the dissipated energy and the internal damage of rock began to grow steadily and rapidly. Compared with uniaxial compression and low confining pressure, the rock has weaker energy hardening and energy accumulation characteristics under high confining pressure state. As presented in Table 2, the elastic energy ratio at stress threshold σ_{eb} decreased with the

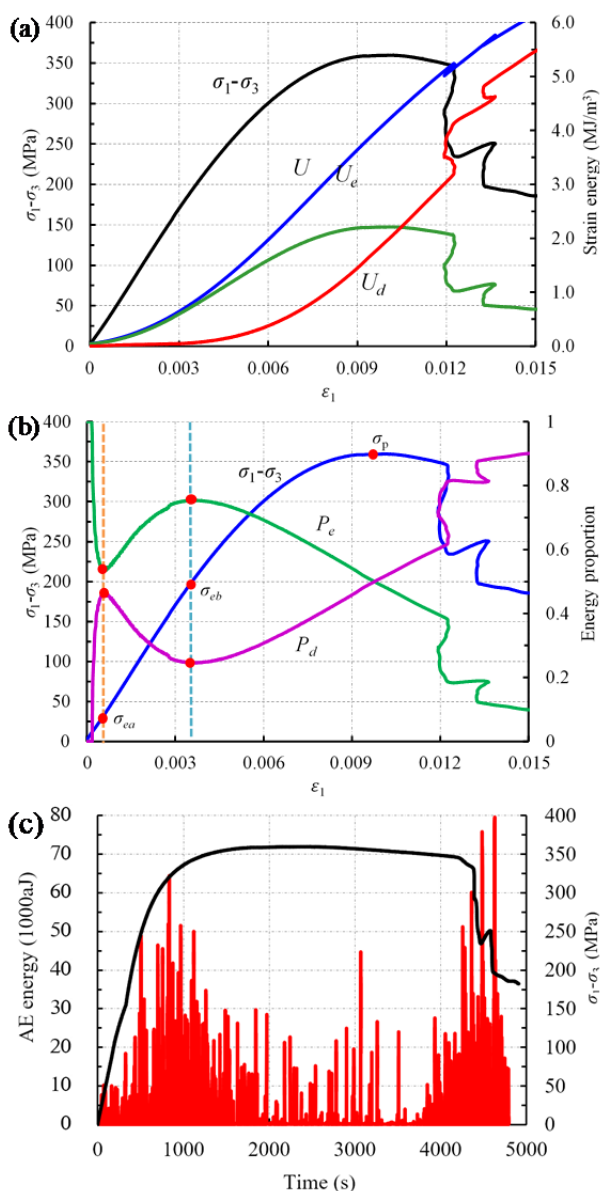


Fig. 12 Progressive damage evolution characteristics of S-40: (a) strain energy; (b) strain energy ratio; (c) acoustic emission.

confining pressure. In S-40, the P_e at σ_{cb} was only 75.3%, whereas it could up to 94.8% under uniaxial compression condition. At the same time, the σ_{cb}/σ_P of S-40 decreased to 53.1%, which was only 64.9% that of D-0. Lower elastic strain energy conversion rate and earlier entering into the energy softening phase indicate that the energy hardening characteristics of the hard-brittle rock in the high confining pressure state was weakened. Furthermore, from σ_{cb} to σ_P , only 40.7% of the total energy could be converting into the elastic energy, whereas it was 75.3% in the previous stage of 0~ σ_{cb} . The results show that

the cracks began to sprout and expand inside of the sandstone, the steady increase of dissipated energy leads to the decrease of rock strength and energy storage capacity. Increasing dissipated energy and its proportion to the total energy reflected the progressive energy damage evolution mechanism of rock. Meanwhile, the increase of dissipated energy reduced the ability of rock to resist failure, while the increase of elastic energy enhanced the ability to drive rock failure. When the two met, the whole rock will be destroyed at the peak strength point of σ_P . Once the rock entered the post-peak phase (σ_{P-}), the accumulated elastic strain energy was released rapidly and the dissipation energy was increased rapidly. Due to 40 MPa confining pressure, the elastic energy after rock failure could maintain a certain residual level, but the dissipated energy was still growing steadily. In this stage, the total energy absorbed by rock was basically used for the further development of rock fracture and shear deformation along the macroscopic failure surface. Compared with uniaxial compression, the compression effect of high confining pressure made the hard-brittle sandstone need more energy for cracks growth and driving rock damage. Hence, the energy index of triaxial compression was much larger than that of uniaxial compression, and increased with the increase of confining pressure. Meanwhile, the increases of dissipated energy and the release of elastic energy of S-40 was not as fast as that of D-0, it had a more significant progressive damage evolution process.

Different damage mechanisms and different energy properties also changed the evolution characteristics of acoustic emission of sandstone after the confine pressure was applied. As presented in Fig. 14c, the AE evolution type of S-40 gradually transition to foreshock-main shock-after shock type. A lot of AE events in the pre-peak and post-peak stages, but the energy level decreases significantly with the increase of confine pressure, the maximum AE energy value of S-40 was only 79.8×10^3 aJ.

The damage of surrounding rock in the process of actual tunnel excavation is induced by dynamic unloading of the initial stress field. Fig. 13 shows the progressive damage evolution characteristics of the hard-brittle sandstone in unloading triaxial compression test of 40 MPa confine pressure. The evolution characteristics of energy curves of X-40 before unloading point were similar to S-40, its elastic energy ratio P_e at stress thresholds σ_{cb} and σ_P were

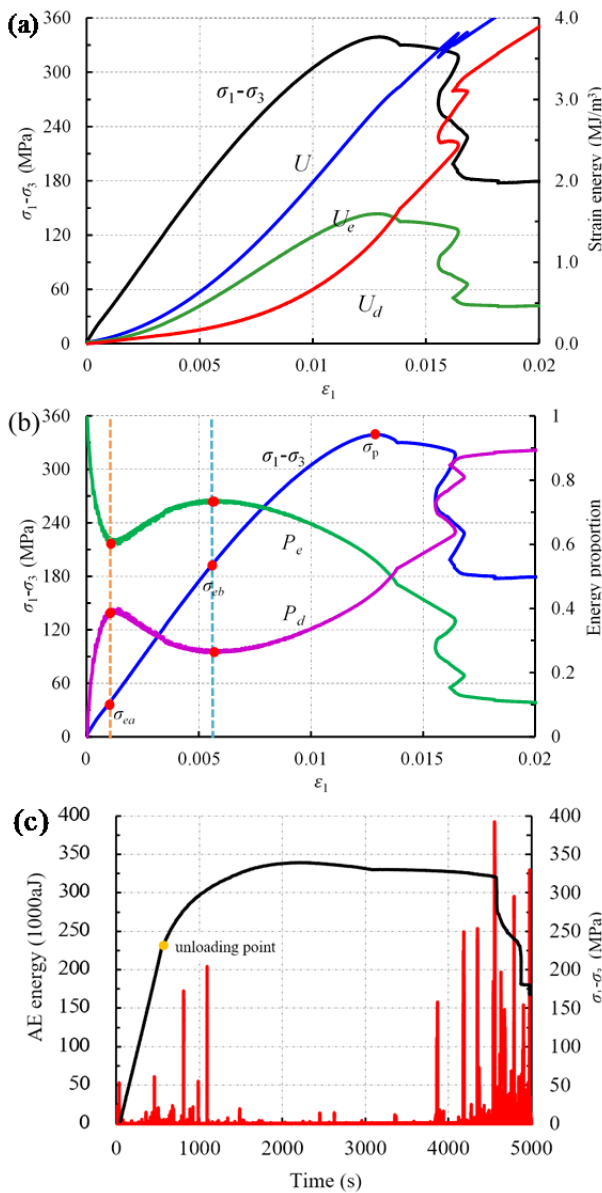


Fig. 13 Progressive damage evolution characteristics of X-40: (a) strain energy; (b) strain energy ratio; (c) acoustic emission.

74.1% and 55.6%, respectively. However, the damage evolution behavior of rock in unloading stage changed significantly when compared with the conventional triaxial test, the X-40 had stronger energy hardening and brittle failure characteristics. Firstly, from σ_{eb} to σ_p , about 54.8% of the total energy could be converting into the elastic energy, which was 14.1% higher than that of S-40 (Table 2). Thus, its growth rate of dissipated energy ratio P_a in the pre peak stage was lower than S-40. Then, the evolution curves of U_a and P_a of X-40 in the rock failure stage was steeper than that of S-40, the rock had stronger elastic release

capacity when under unloading state. Finally, sporadic AE events occurred at the initial unloading stage and then entered a quiet period, whereas there was a large amount of elastic energy release of high energy level in the rock failure stage. The maximum AE energy value of X-40 could up to 391.2×10^3 aJ, which was 4.9 times the S-40.

4.3 Damage evolution rate

In the process of producing, accumulating, rapidly releasing and maintaining a certain residual value of elastic strain energy in rock, its peak point is called the energy storage limit U_{max}^e . As presented in Fig. 14, the energy storage limit increases with the increase of confining pressure, and has a good linear relationship in both conventional triaxial compression and unloading triaxial compression tests. The energy storage limit of D-0, S-20, S-30 and S-40 were 560.1, 1357.0, 1809.8 and 2209.1 KJ/m³, respectively. While the U_{max}^e of X-20, X-30 and X-40 were 1148.9, 1606.0 and 1939.7 KJ/m³, respectively. The energy storage capacity of sandstone in unloading triaxial state was higher than that of uniaxial compression and lower than that of conventional triaxial test. Under high confining pressure condition, the hard-brittle rock can accumulate more releasable elastic strain energy.

According to the above analysis of progressive damage characteristics of rock under different stress paths, the evolution law of elastic energy U_e and dissipated energy U_a can reflect the progressive damage of rock, but the change law of them is opposite. Hence, we define the damage coefficient, D_{de} , to evaluate the damage status of a rock, and it can be calculated using the following equation:

$$D_{de} = \frac{U_d}{U_d^p} \quad (4)$$

where U_d is the dissipated energy at any time, U_d^p is the energy dissipated at peak strength, and $D_{de}=0$ indicates no damage before loading, whereas $D_{de}=1$ means that the rock is totally damaged as it reaches its peak strength.

Taking the damage coefficient evolution characteristics of sandstone in conventional triaxial compression as an example (Fig. 15), the established damage coefficient, D_{de} , could well present the progressive damage characteristics of hard-brittle

Table 2 Energy damage parameters of sandstone under different stress paths

Samples number	σ_{eb}/σ_P (%)	P_e (%)		$\Delta U_e/\Delta U_d$ in $\sigma_{eb}-\sigma_P$ (%)	Maximum AE energy (1000aJ)	AE evolution type	U_{max}^e (KJ/m ³)	R_b	R_a
		at σ_{eb}	at σ_P					(J·m ⁻³ ·s ⁻¹)	
D-0	81.7	94.8	80.3	68.6	689.2	Slight shock-no shock-main shock	560.1	101.3	9817.6
S-20	63.4	82.6	61.6	51.9	269.8	Fore shock-slight shock-main shock	1357.0	449.2	4120.9
S-30	58.6	78.3	52.6	45.9	179.6	Fore shock-main shock-after shock	1809.8	610.2	2471.6
S-40	53.1	75.3	48.5	40.7	79.8	Fore shock-main shock-after shock	2209.1	778.2	1872.5
X-20	64.5	81.9	67.9	61.2	258.6	Foreshock-slight shock-main shock	1148.9	361.0	1036.8
X-30	58.1	77.9	61.3	58.9	318.9	Foreshock-slight shock-main shock	1606.0	549.7	3437.6
X-40	54.2	74.1	55.6	54.8	391.2	Foreshock-no shock-main shock	1939.7	610.2	4725.0

Note: σ_{eb} , stress of rock enters the energy hardening stage; σ_P , peak strength; P_e , elastic strain energy ratio; ΔU_e , increment of elastic energy; ΔU_d , increment of dissipated energy; U_{max}^e , maximum elastic energy; R_b and R_a , slope of dissipated energy before and after peak strength.

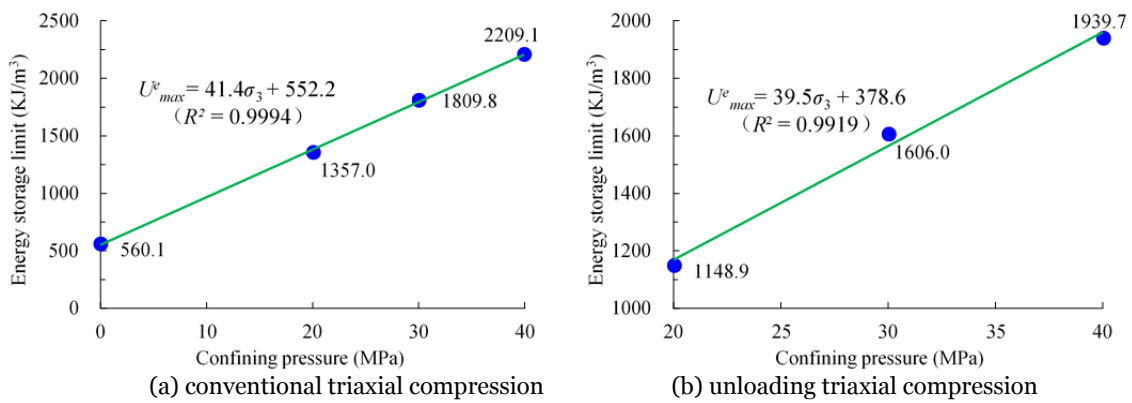


Fig. 14 Relationship curves of energy storage limit (U_{max}^e) and confining pressure (σ_3).

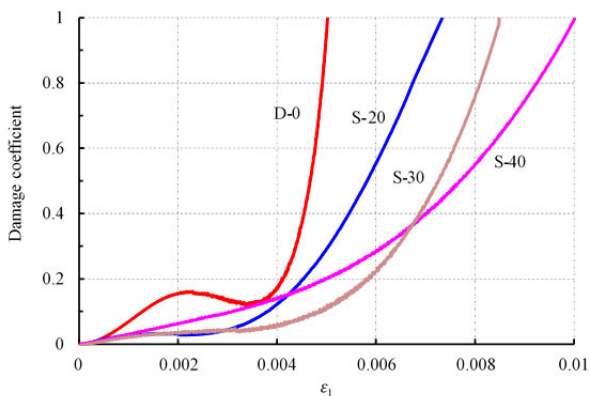


Fig. 15 Damage coefficient evolution characteristics of sandstone in conventional triaxial compression.

rock. Under uniaxial compression test, the initial damage of rock was higher and the damage rate

before peak strength was much faster than that under confining pressure. After confining pressure was applied, the damage evolution process of rock was longer. Moreover, the larger the confining pressure was, the stronger the progressive damage evolution was.

Therefore, the evolution process of dissipated energy can basically show the progressive damage characteristics of rock. Thus, in order to further analyze the influence of stress path on rock damage evolution rate, the evolution curves of strain energy with time of S-40 was drawn and it was presented in Fig. 16. In the early stage of loading, it was the main energy storage phase of rock. Benefit from high confining pressure to improve the energy storage capacity of rock, the U_{max}^e of S-40 was up to 2209.1

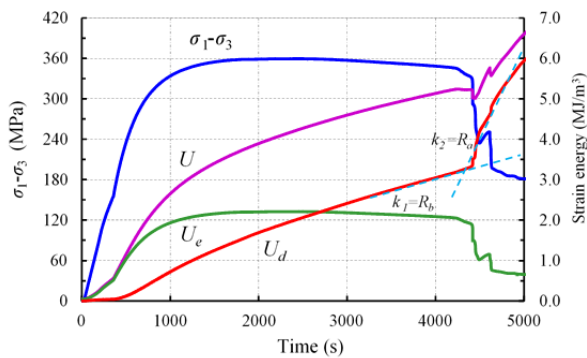
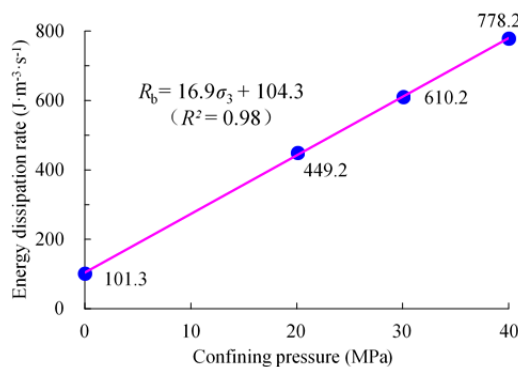


Fig. 16 Evolution curves of strain energy with time of S-40.

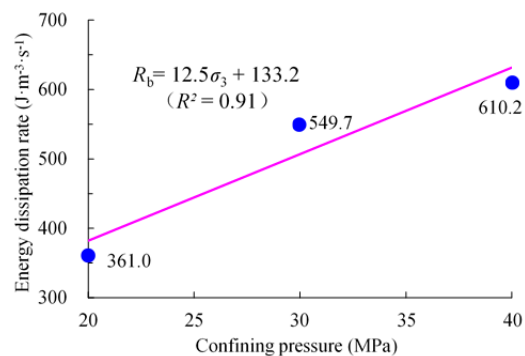
KJ/m³. After more than 500 seconds, the dissipated energy of rock began to increase gradually. In particular, in the pre-peak and post-peak stages of rock, the dissipated energy shown an approximate linear growth law. Hence, we define the slope of dissipated energy before and after peak strength were R_b and R_a , respectively. Meanwhile, the R_b and R_a of sandstone under different stress paths were calculated and presented in Table 2.

Fig. 17 shows the relationship between the energy

dissipation rate and confining pressure before peak strength. The R_b of D-0, S-20, S-30 and S-40 were 101.3, 449.2, 610.2 and 778.2 $J \cdot m^{-3} \cdot s^{-1}$, respectively. Whereas the R_b of X-20, X-30 and X-40 were 361.0, 549.7 and 610.2 $J \cdot m^{-3} \cdot s^{-1}$, respectively. It can be seen that the energy dissipation rate before peak strength increases linearly with the increase of confining pressure under different stress paths. Under the same confining pressure, the damage rates of unloading triaxial state were lower than that of conventional triaxial state. Meanwhile, Fig. 18 shows the relationship between the energy dissipation rate and confining pressure after peak strength. Since the failure stage is the main energy release stage of rock, the R_a is several times of R_b under different stress paths. It shows that the damage rate of rock before the peak strength was small, but after the peak strength was rapid. The sudden steepening of the dissipated energy curve indicates the rock failure occurs. Generally speaking, under the condition of low confining pressure, it is more conducive to the sudden release of rock energy. Thus, the energy dissipation rate of rock under conventional triaxial

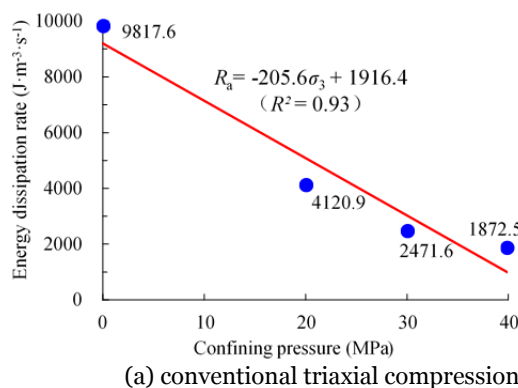


(a) conventional triaxial compression

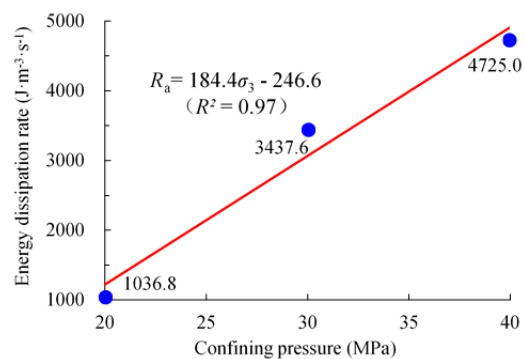


(b) unloading triaxial compression.

Fig. 17 Relationship between the energy dissipation rate (R_b) and confining pressure (σ_3) before peak strength.



(a) conventional triaxial compression



(b) unloading triaxial compression

Fig. 18 Relationship between the energy dissipation rate (R_a) and confining pressure (σ_3) after peak strength.

compression decreases linearly with the increase of confining pressure. The R_a of D-0, S-20, S-30 and S-40 were 9817.6, 4120.9, 2471.6 and 1872.5 $J \cdot m^{-3} \cdot s^{-1}$, respectively. Curiously, the energy dissipation rate of rock under unloading triaxial compression still increases linearly with the increase of confining pressure. The R_a of X-20, X-30 and X-40 were 1036.8, 3437.6 and 4725.0 $J \cdot m^{-3} \cdot s^{-1}$, respectively. High confining pressure is more conducive to the sudden release of energy. This further proves that the unloading stress path will promote the brittle failure of rock.

Overall, under uniaxial compression, the pre-peak damage rate of rock is the smallest, while the post-peak damage rate is the largest. If the confining pressure is increased, the energy storage capacity and the damage rate before the peak strength will be increased, but it will affect the brittleness of rock and reduce the damage rate after peak strength. In unloading state, more energy could be converted into elastic energy in $\sigma_{eb}-\sigma_P$, so the damage rate of rock in unloading state is lower than that in conventional triaxial compression state. Under confine pressure of 20 MPa, the R_a of X-20 is lower than that of S-20. However, with the increases of confining pressure, the post-peak damage rate of rock increases rapidly under unloading condition. The R_a of X-30 is 1.39 times of S-30, while X-40 is 2.58 times of S-40. Therefore, the deep-buried hard-brittle rock with good energy storage capacity can gather a large amount of releasable elastic strain energy. And under the unloading effect of rockmass excavation, it is conducive to the rapid release of elastic, so as to induce brittle fracture of surrounding rock. This is the internal energy damage mechanism of rockburst in the unloading excavation process of hard-brittle rockmass under high ground stress state.

5 Conclusion

In this paper, the cyclic loading-unloading, loading-unloading, uniaxial, conventional and unloading triaxial compression tests on samples of hard-brittle sandstone were conducted. The effect of stress paths and confining pressure on mechanical properties and failure mechanism of rock were systematically discussed. Meanwhile, using energy damage theory and acoustic emission characteristics, the progressive damage evolution characteristics and

evolution rate of rock under different stress paths were analyzed. The main conclusions of this study are as follows:

(1) Increasing the confining pressure was beneficial to improve the mechanical parameters of hard-brittle rock, but it could reduce the brittle failure features. Compared with conventional triaxial compression, the sandstone under unloading state had more remarkable stress drop and unstable failure characteristics.

(2) Compared with uniaxial compression and low confining pressure, the rock had weaker energy hardening and energy accumulation characteristics under high confining pressure state. With the increase of confining pressure, the progressive damage evolution characteristics of rock were enhanced. In unloading state, more energy could be converted into elastic energy in energy softening phase, $\sigma_{eb}-\sigma_P$, so that the pre-peak damage rate of rock was lower than that of conventional triaxial compression state.

(3) The energy storage capacity of rock increases linearly with the increase of confining pressure. Under uniaxial compression, the U_{max}^e of rock was the lowest, followed by unloading state, while under conventional triaxial compression, the rock could gather the highest releasable elastic strain energy.

(4) Energy dissipation and release in the process of rock deformation were the internal power of driven rock progressive damage. The energy dissipation rate of rock after peak strength decreased linearly with the increase of confining pressure under conventional triaxial compression state, while in unloading state it shown the opposite law. This illustrated that the deep-buried rockmass is more likely to induce the brittle failure disaster represented by rockburst under the influence of unloading by surrounding rock excavation.

6 Recommendation

According to the above experimental results, the progressive damage evolution of rockmass was driven by energy dissipation and energy release in the process of rock deformation, and more releasable elastic strain energy could be accumulated under high stress state. At the same time, the brittle fracture mechanism and energy release rate in the failure phase would be strengthened under the unloading stress path. Therefore, in the process of tunnel

excavation in deep-buried hard-brittle rockmass, the rapid unloading of in-situ stress caused by surrounding rock excavation is very easy to induce strong rockburst disaster. With China's tunnel construction and mining resources development entering deep strata, more efforts should be devoted to the failure mechanism and progressive damage of hard-brittle rock. Through the research of this paper, the following suggestions are put forward:

(1) Under the high confining pressure state, the macroscopic failure mode of rock is mainly shear fracture, which means that the support measures for the deep-buried tunnel should be mainly shear failure prevention. Therefore, it is an effective method to reduce the loose zone and deal with the shear failure of surrounding rock by increasing the reasonable spacing and length of system bolts.

(2) For a long time, the full-length adhesive rock bolt system has been widely used in tunnel and underground engineering in China. However, this bolt can not quickly restore the three-dimensional stress state and reduce the stress difference of surrounding rock, it doesn't play a good role in controlling rockburst disaster. Therefore, in order to improve the stress state of surrounding rock and actively mobilize its bearing capacity, the prestressed anchorage system and energy absorbing bolt are suggested to be used in

the future hard-rock tunnel under high geo-stress.

(3) In the process of tunnel excavation, some stress release holes could be drilled to release part of the releasable elastic strain energy stored in the rockmass in advance. In addition, more attention should be paid to the reasonable control of the excavation rate of the surrounding rock and the reasonable construction time of the supporting structures, which should also be considered in the future laboratory tests.

Acknowledgments

This research was supported by the National Natural Science Foundation of China (No. 52008351), the Sichuan Science and Technology Program (No. 2021YJ0539), the project funded by China Postdoctoral Science Foundation (No. 2020TQ0250), the Open Foundation of MOE Key Laboratory of Engineering Structures of Heavy Haul Railway (Central South University) (No. 2020JZZ01) and the Open Foundation of State Key Laboratory of Geohazard Prevention and Geoenvironment Protection (Chengdu University of Technology) (No. SKLGP2021K019).

References

- Barla G, Bonini M, Semeraro M (2011) Analysis of the behaviour of a yield-control support system in squeezing rock. *Tunn Undergr Space Technol* 26(1): 146-154. <https://doi.org/10.1016/j.tust.2010.08.001>
- Cantiati L, Anagnostou G (2009) The effect of the stress path on squeezing behavior in tunneling. *Rock Mech Rock Eng* 42: 289-318. <https://doi.org/10.1007/s00603-008-0018-9>
- Chen ZQ, He C, Wu D, et al. (2017) Fracture evolution and energy mechanism of deep-buried carbonaceous slate. *Acta Geotech* 12(6): 1243-1260. <https://doi.org/10.1007/s11440-017-0606-5>
- Chen ZQ, He C, Ma GY, et al. (2019) Energy damage evolution mechanism of rock and its application to brittleness evaluation. *Rock Mech Rock Eng* 52: 1265-1274. <https://doi.org/10.1007/s00603-018-1681-0>
- Cui Z, Sheng Q, Leng X, Ma YL (2019) Investigation of the long-term strength of Jinping marble rocks with experimental and numerical approaches. *Bull Eng Geol Environ* 78(2): 877-882. <https://doi.org/10.1007/s10064-017-1132-2>
- Diederichs MS, Kaiser PK, Eberhardt E (2004) Damage initiation and propagation in hard rock during tunnelling and the influence of near-face stress rotation. *Int J Rock Mech Min Sci* 41: 785-812. <https://doi.org/10.1016/j.ijrmms.2004.02.003>
- Dwivedi RD, Singh M, Viladkar MN, Goel RK (2013) Prediction of tunnel deformation in squeezing grounds. *Eng Geol* 161: 55-64. <https://doi.org/10.1016/j.enggeo.2013.04.005>
- Feng XT, Yu Y, Feng GL, et al. (2016) Fractal behaviour of the microseismic energy associated with immediate rockbursts in deep, hard rock tunnels. *Tunn Undergr Space Technol* 51: 98-107. <https://doi.org/10.1016/j.tust.2015.10.002>
- Huang D, Li YR (2014) Conversion of strain energy in triaxial unloading tests on marble. *Int J Rock Mech Min Sci* 66: 160-168. <https://doi.org/10.1016/j.ijrmms.2013.12.001>
- Hua AZ, You MQ, 2001. Rock failure due to energy release during unloading and application to underground rock burst control. *Tunn Undergr Space Technol* 16: 241-246. [https://doi.org/10.1016/S0886-7798\(01\)00046-3](https://doi.org/10.1016/S0886-7798(01)00046-3)
- Khazaei C, Hazzard J, Chalaturnyk R (2015) Damage quantification of intact rocks using acoustic emission energies recorded during uniaxial compression test and discrete element modeling. *Comput Geotech* 67: 94-102. <https://doi.org/10.1016/j.compgeo.2015.02.012>
- Li DY, Sun Z, Xie T, et al. (2017) Energy evolution characteristics of hard rock during triaxial failure with different loading and unloading paths. *Eng Geol* 228: 270-281. <https://doi.org/10.1016/j.enggeo.2017.08.006>
- Lim A, Ou CY (2017) Stress paths in deep excavations under undrained conditions and its influence on deformation analysis. *Tunn Undergr Sp Tech* 63: 118-132. <https://doi.org/10.1016/j.tust.2016.12.013>
- Liu GF, Feng XT, Feng GL, et al. (2016) A method for dynamic risk assessment and management of rockbursts in drill and blast tunnels. *Rock Mech Rock Eng* 49(8): 3257-3279.

- <https://doi.org/10.1007/s00603-016-0949-5>
Li TB, Ma CC, Zhu ML, et al. (2017) Geomechanical types and mechanical analyses of rockbursts. *Eng Geol* 222: 72-83.
<https://doi.org/10.1016/j.enggeo.2017.03.011>
- Li XB, Cao WZ, Zhou ZL, Zou Y (2014) Influence of stress path on excavation unloading response. *Tunn Undergr Space Technol* 42: 237-246.
<https://doi.org/10.1016/j.tust.2014.03.002>
- Ma CC, Li TB, Xing HL, et al. (2016) Brittle rock modeling approach and its validation using excavation-induced microseismicity. *Rock Mech Rock Eng* 49(8): 3175-3188.
<https://doi.org/10.1007/s00603-016-0941-0>
- Ma CC, Li TB, Zhang H (2020) Microseismic and precursor analysis of high-stress hazards in tunnels: A case comparison of rockburst and fall of ground. *Eng Geol* 265: 10543.
<https://doi.org/10.1016/j.enggeo.2019.105435>
- Martin CD, Chandler NA (1994) The progressive fracture of Lacdu Bonnet granite. *Int. J. Rock Mech. Min Sci Geomech Abstr* 31: 643-659.
[https://doi.org/10.1016/0148-9062\(94\)90005-1](https://doi.org/10.1016/0148-9062(94)90005-1)
- Munoz H, Taheri A, Chanda EK (2016) Rock drilling performance evaluation by an energy dissipation based rock brittleness index. *Rock Mech Rock Eng* 49(8), 3343-3355.
<https://doi.org/10.1007/s00603-016-0986-0>
- Xiao YX, Feng XT, Li SJ, et al. (2016) Rockmass failure mechanisms during the evolution process of rockbursts in tunnels. *Int J Rock Mech Min Sci* 83: 174-181.
<https://doi.org/10.1016/j.ijrmms.2016.01.008>
- Xie HP, Ju Y, Li LY (2005) Criteria for strength and structural failure of rocks based on energy dissipation and release principles. *Chin J Rock Mech Eng* 24: 3003-3010. (In Chinese) <http://orcid.org/0000-0002-1686-7827>
- Xu H, Feng XT, Yang CX (2019) Influence of initial stresses and unloading rates on the deformation and failure mechanism of Jinping marble under true triaxial compression. *Int J Rock Mech Min Sci* 117: 90-104.
<https://doi.org/10.1016/j.ijrmms.2019.03.013>
- Yan P, Lu W, Chen M, et al. (2015) Contributions of in-Situ stress transient redistribution to blasting excavation damage zone of deep tunnels. *Rock Mech Rock Eng* 48: 715-726.
<https://doi.org/10.1007/s00603-014-0571-3>
- Yang SQ (2016) Experimental study on deformation, peak strength and crack damage behavior of hollow sandstone under conventional triaxial compression. *Eng Geol* 213: 11-24.
<https://doi.org/10.1016/j.enggeo.2016.08.012>